

Flow Velocity and Travel Time Determination on Grid Basis Using Spatially Varied Hydraulic Radius

M. A. Gad*

Irrigation and Hydraulics Laboratory, Civil Engineering Department, Faculty of Engineering, Ain-Shams University, Cairo, Egypt 11566

Received 14 March 2012; revised 2 July 2012; accepted 15 October 2013; published online 11 June 2014

ABSTRACT. The hydraulic radius has always been a difficult variable to be estimated using the available data for ungauged flood routes, especially if grid-based calculations are used. This difficulty arises since the available digital elevation models are usually of poor resolution to describe the cross sectional details especially in arid and semiarid regions. This research develops a new grid-based technique to estimate travel time using spatially varied hydraulic radius. The technique implements the stream power formulation to relate the hydraulic radius R at any cross section to the hydrologic parameters of the upstream catchment area. A spatially varied grid-based Manning's formula is used to determine flow velocity from the calculated hydraulic radius. Many anticipated uses of the developed technique are expected.

Keywords: grid, velocity, hydraulic radius, rainfall, runoff, modeling, watershed, GIS

1. Introduction

Flow velocity and travel time are key variables in many water resources applications including rainfall-runoff modeling. For a watershed system, the shape of the hydrograph and the peak discharge depend on the arrival times of the system components. For example, the peak discharge increases when the arrival times of the system components coincide at the outlet and the opposite is true. Without exception, all rainfall-runoff models require an estimate of the travel time through the catchment area. This includes the rational method (Nyarko, 2002), lumped and distributed unit hydrograph models (Gross and Moglen, 2007), the semi-distributed and time-area models (Ajward and Muzik, 2000), and the distributed rainfall-runoff models (Jain et al., 2004). Although distributed/hydrodynamic models can provide travel time as output (not input), but such models are still not practical for engineering applications. This is because of the very high resolution digital elevation models (DEMs) that are required to describe details of the hydraulic cross section, the significant run-time requirements, and the uncertainty in the hydraulic boundary conditions. Hundreds of empirical formulas are available to calculate the time of concentration (T_c) from topographic and/or rainfall characteristics (Wanielista et al., 1997; Sharifi and Hosseini, 2011). These for-

mulas can be applied in a time-consuming manual mode, automated lumped mode, or automatic grid-based mode. In the last two decades, the automatic grid-based mode took much attention for the following reasons:

1. The Shuttle Radar Topography Mission (SRTM) gridbased elevation data constitutes now the main source of topography in hydrologic modeling worldwide with an average resolution of 100 m depending on the location on the Earth. A new generation of SRTM data is currently available with 30 m resolution in many parts of the Earth.
2. The first mode (i.e., the manual mode) is approximate and subject to human error. In addition, it consumes a considerable and costly time. The second mode (i.e., the automated lumped mode) suffers from zonal averaging approximations in dealing with grid data. These zonal averaging operations are required to determine a single hydrologic feature (e.g., slope or roughness) for each single hydrologic element such as a sub-catchment or reach (ESRI, 2006; HEC, 2010).
3. The semi-distributed models, time-area models, and distributed models require an estimate of travel time directly in grid format.
4. To facilitate the incorporation of high resolution gauge and radar rainfall data (Seo and Smith, 1992; Tsanis and Gad, 2003; and others) in hydrologic modeling applications (nowcasting for example).

For the above reasons, this study focuses on the automatic grid-based calculations of travel time (note that the findings of this research are also applicable to the other two modes). Grid-based implementation of the available T_c equations encounters

* Corresponding author. +2 0100 5293387; fax: +2 026830947.
E-mail address: hydroshams@yahoo.ca (M. A. Gad).

main problems in semiarid regions that can be summarized as follows:

1. In semiarid mountainous regions, the level of excess rainfall has a significant effect on the time of concentration. For example, lag-analysis of the observed hyetographs/hydrograph data, collected by EL-Sayed and Habib (2008) in Wadi Sudr in Egypt, shows that T_c changes from storm to storm being significantly less in intense storms. The storm-dependant time of concentration has also been reported in different studies worldwide indicating that it can not be treated as a unique/constant hydrologic feature for a watershed (Rao and Delleur, 1974; Thomas et al., 2000). Most of the available T_c equations are incapable of considering the intensity of precipitation. In addition, water quality studies seek the low flow condition and not the high flow condition simulated by most of the available travel time formulas.
2. The nonlinearity associated with the discretization of the channel length in these formulas (i.e., subdividing a stream into more parts will not yield the same calculated time of concentration). Hence, this non-linearity in length adds more dependency on the grid resolution (grids of different resolutions yield significantly different travel times).

2. Problem Formulation

Many researchers have attempted practical grid-based calculations of travel time using different approaches. A comprehensive summary of previous research is presented in Du et al. (2009). Maidment (1993) used a velocity equation that is based on slope and landuse (Sircar et al., 1991) to calculate the travel time grid. Dervos et al. (2006) split the calculations into overland flow and channel flow. They implemented the kinematic wave approximation in overland flow (Overton and Meadows, 1976) while channel flow velocities were taken constants and estimated based on calibration with observed hydrographs. The non-linear length in the kinematic wave approximation is avoided in their work using the lumped automated approach (refer to the introduction). Ajward and Muzik (2000) tried to include discharge-dependant travel time calculations. The discharge is pre-calculated for each pixel in terms of the upstream area (i.e., from the flow accumulation value). Manning's equation is then solved in each pixel for the average water depth, and consequently the velocity of flow is determined. Channel widths are estimated in this technique from aerial photographs causing a degree of uncertainty. In addition, the pre-calculation of discharge in each pixel involves substantial approximation since it is usually based on simplified calculations (e.g., the rational method). However, if detailed information is available for the channel cross sections, this approach can constitute a promising approach. Chiang et al. (2004) followed a similar idea to that of Ajward and Muzik (2000) in developing a time-area instantaneous unit hydrograph. Du et al. (2009) reproduced the discharge-dependent travel time idea described above. They overcame the channel width problem by using the approximation proposed by Kouwen et al. (1993) and Arora et al.

(2001). This approximation assumes that the hydraulic radius (R) is a function of the channel cross sectional area (A_{x-sec}). This way Manning's formula is solved for the channel cross sectional area and consequently the velocity of flow at each pixel is obtained (note that the assumption here is $R = f(A_{x-sec})$). This assumption imposes limitation since it applies only to wide sections and most of the upper streams in semiarid regions depart from this assumption.

In summary, it can be concluded that grid-based calculations of travel time is very important in hydrologic modeling. In addition, previous work proposed different approaches to tackle this problem. Some of these approaches are incapable of considering the level of rainfall intensity. The other approaches, that can consider storm intensity, are based on some assumptions to overcome the lack of channel cross sectional data. These assumptions involve some approximations that may be improved to suit semiarid regions. This research seeks this improvement on the geomorphology-hydrology interface.

3. The Stream Power Principle

The stream power principle makes use of the concept of downstream hydraulic geometry first introduced by Leopold and Maddock (1953). It is widely used in river incision studies (Howard, 1998; Sklar and Dietrich, 1998; Stock and Montgomery, 1999; Whipple and Tucker, 1999; Finlayson and Montgomery, 2003). The stream power laws implement power law relationships between the discharge of a river, Q , and river parameters, v , such as channel width, depth, or longitudinal slope:

$$v = cQ^d \quad (1)$$

where c and d are fitting parameters. Since discharge is a function of drainage area, it is a common practice in grid-based applications to express river parameters in terms of the catchment area A_{us} :

$$v = cA_{us}^d \quad (2)$$

The use of stream power laws in grid based analysis has the advantage that river parameters such as width and depth are rendered independent of the spatial resolution of the DEM (Digital Elevation Model). Many studies have shown that the hydraulic geometry equations perform acceptably for both alluvial and mountainous rivers (e.g., Leopold and Maddock, 1953; Carlston, 1969; Montgomery and Gran, 2001; Kobor and Roring, 2004). These studies showed a good correlation between channel geometry (width or longitudinal slope) and the upstream catchment area. Accordingly, this research inspects the stream power principle in grid-based travel time calculations and extends the predictors to include the upstream excess rainfall and upstream average slope in a trial to improve the prediction. In addition, the research considers a new response that, according to the best knowledge available, has not been fitted to stream-power laws. This new response is the hydraulic radius.

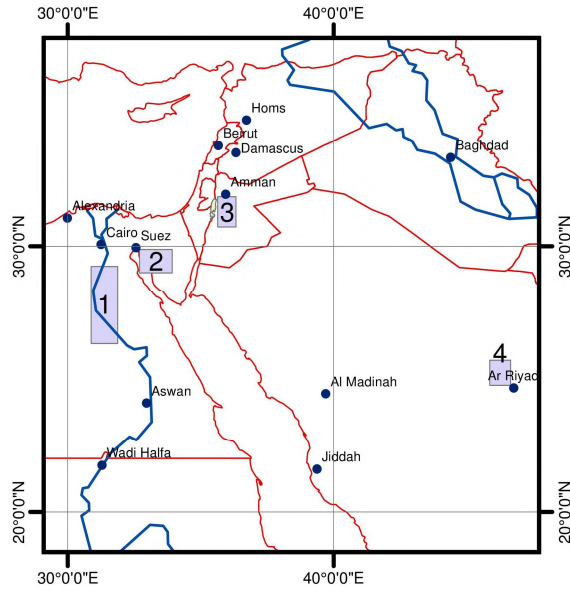


Figure 1. Locations of four regions considered in this study.

4. Modeling the Hydraulic Radius

This section presents the non-linear regression followed in the development of the hydraulic radius formulation and its grid-based implementation. It should be noted that other geomorphologic parameters (width, depth, and slope) were also tested as responses in the preparation stages of this research. Although significant correlations were found between these variables and the predictors, the hydraulic radius showed superior fit and hence it was selected as a response in this research.

4.1. Fitting to a Stream Power Formulation

The hydrologic parameters used to predict the hydraulic radius are the upstream catchment area (A_{us}), the daily areal upstream excess rainfall depth (P_{e-us}), and the upstream average slope (S_{us}). Hence, the proposed form is as follows:

$$R = CA_{us}^n P_{e-us}^m S_{us}^k \quad (3)$$

where R is the hydraulic radius and C is a constant. The daily excess rainfall depth is used here instead of the rainfall intensity in order to suit many applications. This is because the daily depth is used in hydrologic design, continuous simulations, and flood forecasting. It is a typical output of numerical weather prediction models and is estimated from radar rainfall data on both the mesoscale and synoptic scale. In addition, rainfall intensity in semiarid regions is highly correlated with the daily excess depth since higher/lower intensities are associated with higher/lower excess daily depths. In order to explore the relation between the hydraulic radius and its predictors, hydrologic data from eight natural watersheds from four different regions in the Middle East is collected. The four regions are Upper Egypt, Sinai (Egypt), east of the Dead Sea (Jordan), and north of Riyadh City (KSA). The eight Wadies are Al-Mashkak

(Menia, Egypt), Tag El-Der (Suhag, Egypt), El-Meliha (Sinai, Egypt), Zerqa Main (Jordan), Salboukh (Riyadh, KSA), and additional three small catchment areas from South Egypt. The natural catchment areas range from 2 to 500 km² and are characterized with a wide range in topography, land cover, and rainfall extremes. Figure 1 shows the locations of the four regions while their general hydrological characteristics are given in Table 1. The exploring procedure involves preparing a rainfall-runoff data set of storm excess rainfall, watershed hydrologic parameters, and the corresponding peak discharges at certain surveyed cross sections where the hydraulic radius can be estimated from Manning’s formula. Since observed rainfall-runoff data is not sufficiently available in the region, the data set is artificially prepared via hydrologic modeling using HEC-1 package (HEC, 1973). The calculated peak discharges are then plugged into Manning’s formula at the surveyed cross-sections to calculate the hydraulic radius. The calculated hydraulic radius (i.e., the response) can then be related to its predictors (i.e., A_{us} , P_{e-us} , S_{us}) using non-linear regression. The development of the hydraulic radius formula through non-linear regression is described in details in the following steps:

Table 1. General Descriptions of the Regions Studied

Region	Slope	LC	P _{24hr-100yr}
1	Very Mild	Sandstone	40 mm
2	Steep-Mild	Limestone	50 mm
3	Steep	Variable	100 mm
4	Mild	Sandstone	70 mm

1. Rainfall-runoff modeling is performed for all watersheds using HEC-1 detailed networks. The catchment areas are sub-divided into smaller sub-catchments as needed to describe as close as possible the real transforming behavior of the watershed under consideration and to conform to the assumption of spatial uniformity of the parameters. The standard 24 hrs Soil Conservation Services (SCS) type-II design storm (typically used for design purposes) is used to distribute the storm total rainfall depths. The standard SCS type-II storm distribution (SCS, 1973) simulates the typical thunderstorm activities experienced in the Middle East (the common flood producing type). The SCS curve number (CN) loss rate method (SCS, 1972) is used for excess hyetograph estimation and the transformation into runoff hydrographs is accomplished using the SCS dimensionless unit hydrograph method (SCS, 1972). CN values are set based on Landsat images and previous calibration studies (Sorman et al., 1990; Walters, 1990; Abdelrahman, H., 1992; Fahmy, 1992; Gad, 1996). The lag unit hydrograph parameters are taken as 0.6 the time of concentrations estimated using Kirpich’s equation (Kirpich, 1940). The lag method is implemented for routing through the network reaches. It should be noted that this modeling procedure is the most widely used for hydrologic design on the engineering level in the Middle East. HEC-1 simulations are repeated for 11 levels of the storm total rainfall depth (20, 40, 60, 80, 100, 120, 150, 180, 200, 300, and

500 mm). Hence, the corresponding peak discharges (Q_p) are estimated at the surveyed cross sections of each watershed. The levels of the total rainfall depth and the number of cross-sections considered for each watershed expand the number of rainfall-runoff pairs to 94. (i.e., 94 detailed HEC-1 simulations were made).

2. Manning’s formula is solved for channel depth and the hydraulic radius (R) is then obtained. Accordingly, a data set of A_{i-us} , P_{e-us} , S_{i-us} , Q_p , and the corresponding hydraulic radius (R) containing 94 rows is made ready for nonlinear regression.
3. The hydraulic radius (R) is fitted to the predictors using non-linear regression. The predictors are introduced one by one and the extra reduction in the errors sum of squares is evaluated to assess the contribution of each of the three parameters in explaining the response.

Seven combinations (i.e., models) of the three parameters are attempted. The results of the subsets regression are shown in Table 2. As shown in the table, model no.4 (2-predictors model) and model no.7 (3-predictors model) have the best fit. The two models are as follows:

$$R = 0.072 A_{i-us}^{0.23} P_{i-e-us}^{0.53} \tag{4}$$

$$R = 0.1 A_{i-us}^{0.23} P_{i-e-us}^{0.45} S_{i-us}^{0.028} \tag{5}$$

where R_i = hydraulic radius at grid cell i (m); A_{i-us} = accumulated area upstream grid cell i (km^2); P_{i-e-us} = daily excess rainfall depth upstream grid cell i (mm); S_{i-us} = upstream average slope (%). Figure 2 presents a comparison between the hydraulic radius calculated via Manning’s formula and the hydraulic radiuses calculated using the stream power equations for the data set used in the training where Figure 3 and Figure 4 present the sensitivity of the developed stream power equations.

Table 2. Statistics of Best Subsets Regression

Model	A_{us}	P_{e-us}	S_{us}	R^2 (%)
1	×			26.2
2		×		65.4
3			×	20
4	×	×		97.9
5	×		×	26.2
6		×	×	92.8
7	×	×	×	99.42

4.2. Verification

Three cases are used to verify the developed stream power equations. The three cases are the Blue Nile (Ethiopia-Sudan), Wadi El-Arish (Sinai, Egypt), and Wadi Sudr (Sinai, Egypt). The first two cases are beyond the training range used in developing the stream power equations. It should be noted that additional verification through hydrologic modeling is presented in Gad (2013).

The Blue Nile catchment area upstream Khartoum city (Sudan) extends to middle Ethiopia totaling a figure of 320,000

km^2 , the average areal excess rainfall in one day during August to September period is around 5 ~ 7 mm. The longitudinal slope at Khartoum is about 1.2 m/km and the river has non-wide section (Abdo et al., 2009). Plugging this information into the stream power equations yields a flow velocity of 2.6 ~ 2.9 m/s which is similar to the recorded flood velocity at this location (DAR, 2006).

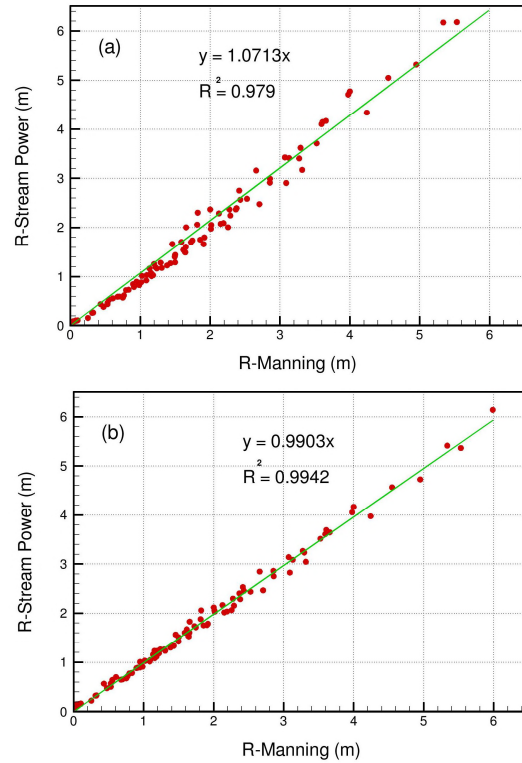


Figure 2. The hydraulic radius obtained from Manning’s formula (X-axis) versus the hydraulic radius calculated from the stream power models (Y-axis) for the cases used in regression. (a) 2-predictors model [A_{us} and P_{e-us}]; (b) 3 predictors model [A_{us} , P_{e-us} , and S_{us}].

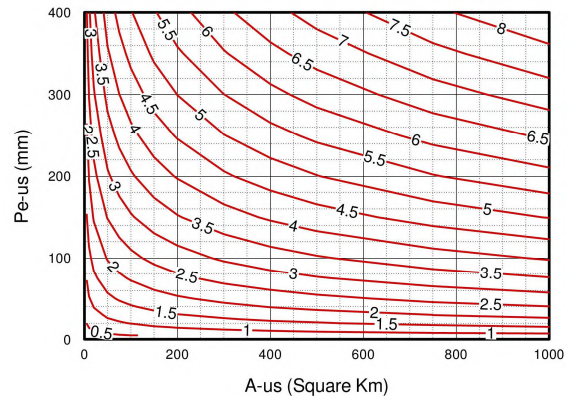


Figure 3. Contours of hydraulic radius (m) at different levels of the upstream catchment area (km^2) and upstream average excess rainfall (mm) using the 2-predictors stream power model. The figure represents the sensitivity due to changes in the predictors.

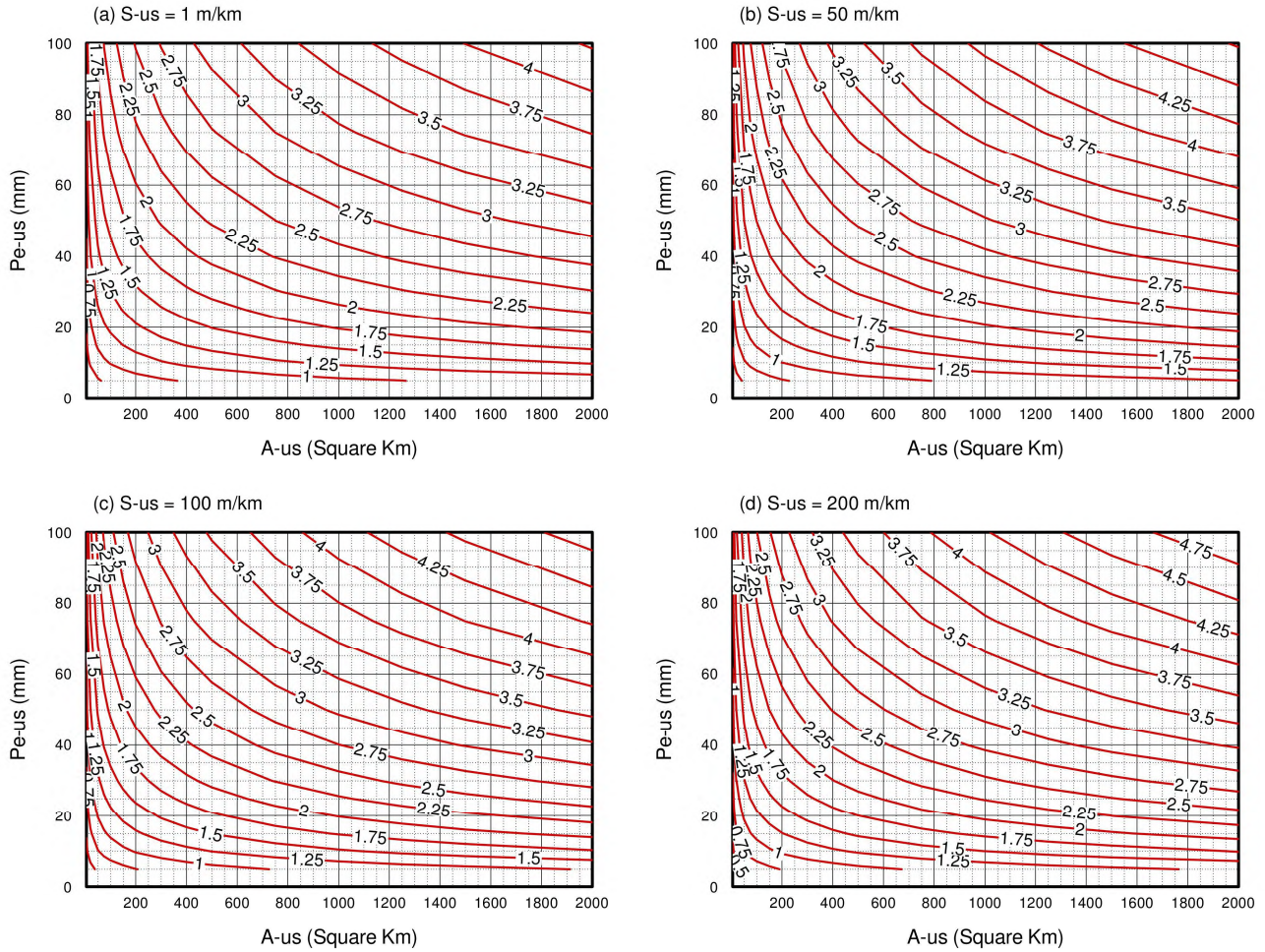


Figure 4. Contours of hydraulic radius (m) at different levels of the upstream catchment area (km²), upstream average excess rainfall (mm), and upstream average slope (m/km) using the 3-predictors stream power model. The figure represents the sensitivity due to changes in the predictors.

Wadi El-Arish is a very large catchment area ($A_{us} = 20,000 \text{ km}^2$ and $S_{us} = 3.5\%$) that originates from the heights of South Sinai and flows northward across North Sinai until it discharges into the Mediterranean. Wadi El-Arish received a severe storm in February 1975. Detailed data of this event was documented and is presented in Klien (1999). The average areal total rainfall depth was 45 mm and the observed peak discharge was 1,650 m³/s. The measured volume of the hydrograph revealed an average areal excess rainfall of 6 ~ 6.75 mm. The average observed width of the flooded channel near the outlet was 500 m and the observed water depth was about 4 m. Substituting the area, excess rainfall, and upstream slope into the stream power equations yields a hydraulic radius of 3.84 ~ 4.05 m which is very consistent with the observed data.

Wadi Sudr is a mid-size catchment ($A_{us} = 600 \text{ km}^2$ and $S_{us} = 9\%$) that originates from the heights of South Sinai and flows west to discharge into the Gulf of Suez. A rainfall storm occurred on March, 22, 1991 and developed a total rainfall of 34.5 mm. The hydrograph peak and volume near the outlet were 265 m³/s and 2.42 million.m³. The corresponding areal excess rainfall is 4.5 mm. The flood width was about 50 m

with an average Manning’s water depth of 0.97m and a hydraulic radius of approximately 0.94 m (EL-Sayed and Habib, 2008). The hydraulic radius from the stream power equations is 0.91 m.

5. Grid-Based Calculations in GIS

A GIS module of grid math, conditioning, cell-to-cell programming, and hydrologic operations is developed in order to automate the calculation of the hydraulic radius, slope, velocity, and travel time on grid basis. The following subsections describe in details this module. Example implementation in rainfall-runoff hydrologic modeling is presented in Gad (2013).

5.1. Grid-Based Calculations of the Hydraulic Radius

The accumulated upstream area in Equations (4) and (5) is calculated by:

$$A_{i-us} = \sum_{i=1}^{i=N_i} a = N_i a = (FA_i + 1) a \tag{6}$$

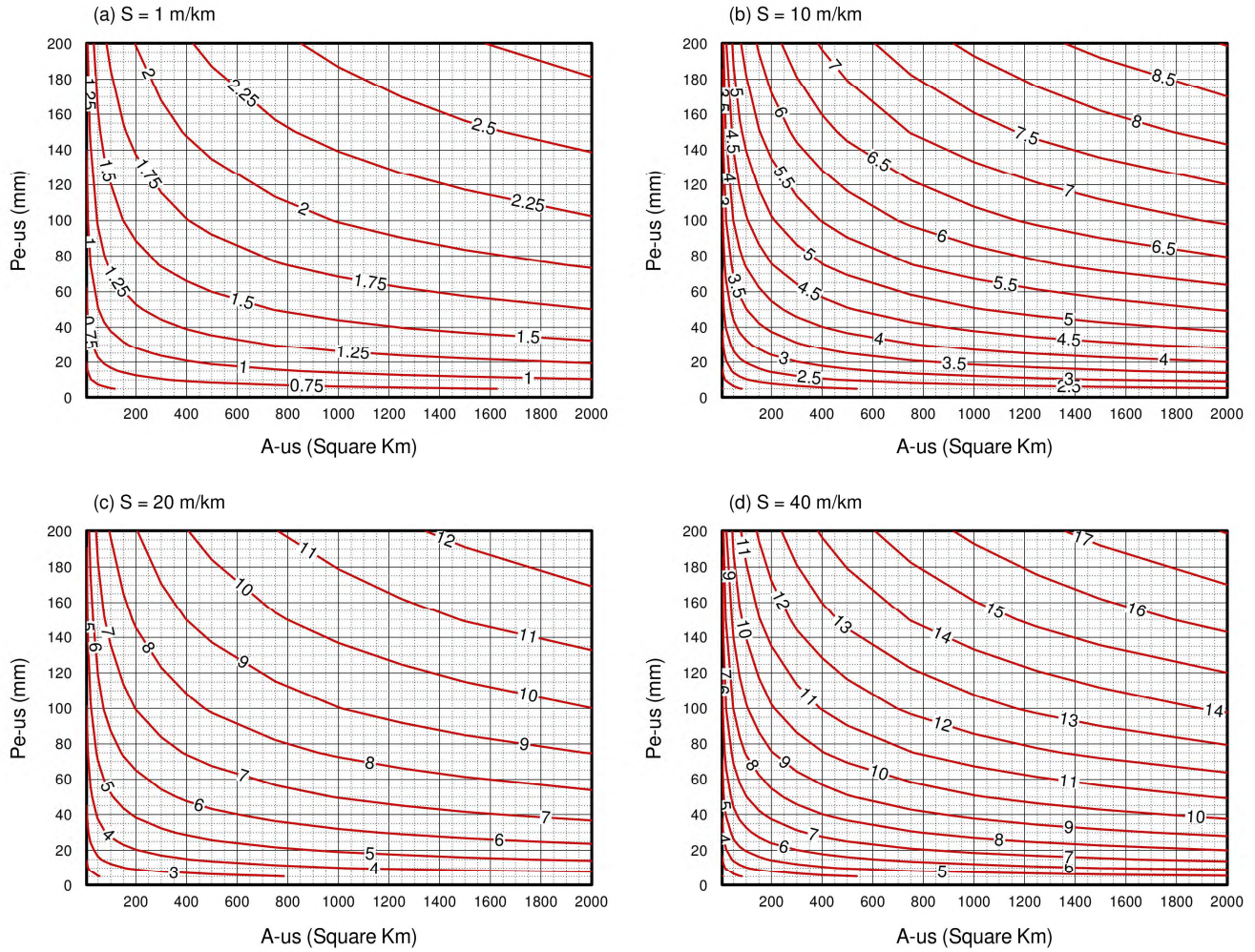


Figure 5. Example Manning's velocity contours (m/s) at different levels of the predictors using the hydraulic radius calculated from the 2-predictors stream power model (Manning's $n = 0.04$). Note that S is the longitudinal slope (not the upstream average slope).

where N_i is the number of upstream grid cells contributing at cell i (including cell i) and a is the area of a grid cell (a constant value = $\text{cellsize}^2 \times 10^{-6}$, where, cellsize is in meters). FA_i denotes the flow accumulation value at cell i obtained from the FlowAccumulation function (available in ESRICORE library). One is added to FA_i because the flow accumulations calculated using the FlowAccumulation function starts from zero (i.e., does not include the area of cell i). The procedure uses the same FlowAccumulation function to determine the average upstream excess rainfall by using a weight grid of excess rainfall. To explain this procedure, consider a storm of total rainfall depth P_i (mm) at any cell i . Let us consider the SCS method for infiltration (SCS, 1972) where CN values are spatially varied and given in a curve number grid (CNGrid), where CN_i denotes the curve number value at cell i . A storage grid is calculated by applying the following equation (SI units) using grid math (i.e., cell by cell math):

$$S_i = \frac{25400 - (254CN_i)}{CN_i} \quad (7)$$

where S_i denotes soil storage at cell i in millimeters. Similarly, grid math and grid conditioning are used to calculate an excess rainfall grid (PeGrid):

$$Pe_i = \begin{cases} \frac{(P_i - (0.2S_i))^2}{P_i + (0.8S_i)} & (\text{if } P_i > 0.2S_i) \\ 0 & (\text{if } P_i \leq 0.2S_i) \end{cases} \quad (8)$$

where Pe_i denotes the excess rainfall depth at cell i (mm). The volume of excess rainfall upstream cell i (VolUsGrid) is obtained by summing excess rainfall volume in all upstream cells:

$$VolUs_i = a \sum_{Upstream} Pe_i = VA_i \times a + (Pe_i \times a) \quad (9)$$

where VA_i denotes the weighted flow accumulation value at cell i obtained from the weighted FlowAccumulation function using the excess rainfall (obtained from Equation 8) as a weight. Note that $(Pe_i \times a)$ is added to VA_i because the weighted

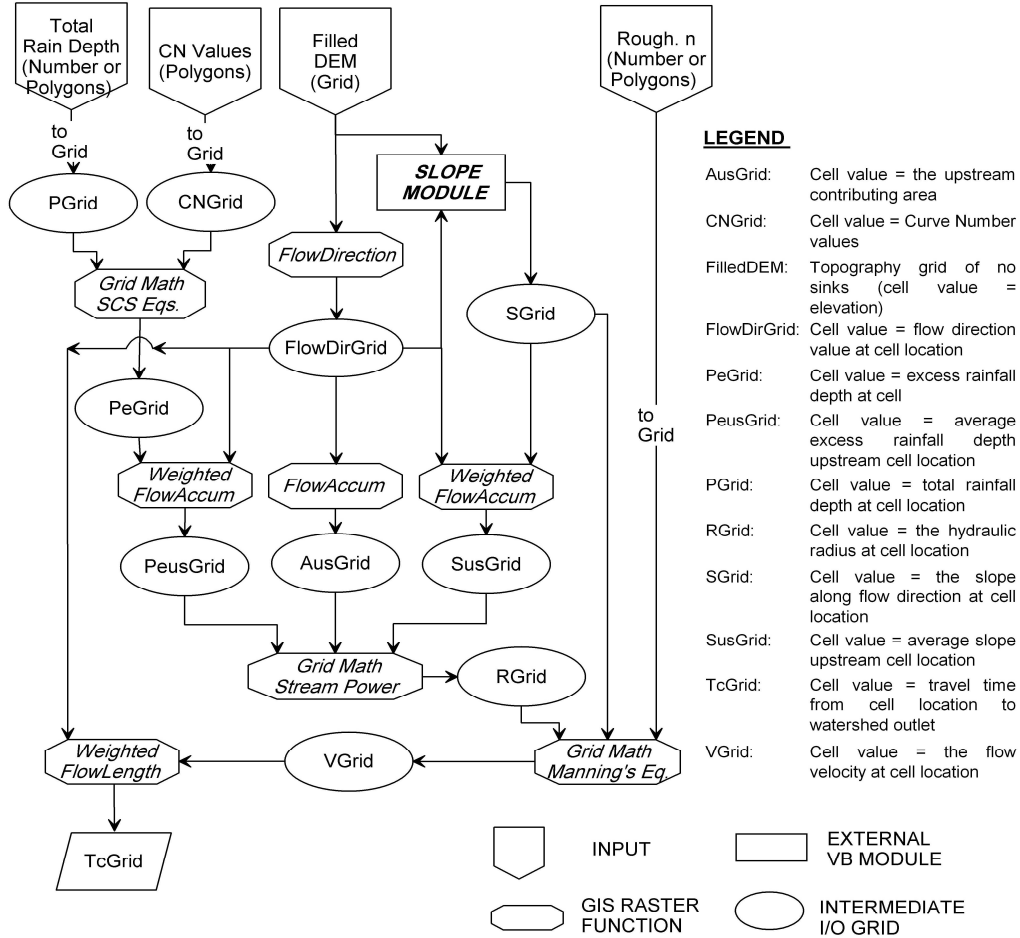


Figure 6. Implementation of the developed stream power formula in GIS. The diagram explains a GIS module to determine a travel time grid (TcGrid) from a DEM. The shown module is a simple module that can easily be incorporated into hydrologic modeling. A useful example of the use of this module in hydrologic modeling can be found in Gad (2013).

flow accumulations calculated using the FlowAccumulation function starts from zero (i.e., does not include the excess rain of cell i). A grid of the average upstream excess rainfall (PeUsGrid) is calculated by dividing Equation (9) by Equation (6):

$$P_{i-e-us} = \frac{VolUS_i}{A_{i-us}} = \frac{VA_i \times a + (Pe_i \times a)}{(FA_i + 1) a} = \frac{VA_i + Pe_i}{FA_i + 1} \quad (10)$$

Similarly, the average upstream slope is determined by the weighted FlowAccumulation function using the longitudinal slope as weight. The hydraulic radius grid (RGrid) can now be calculated by substitution into Equation (4) or (5) using grid math.

5.2. Velocity and Travel Time

Manning's formula (Manning 1891) is implemented to estimate flow velocity on grid basis (VGrid). For simplicity, Manning's formula is used here to cover both overland flow and channel flow. Substituting the hydraulic radius from Equa-

tion (4) or (5) into Manning's formula yields the velocity of flow as follows:

$$V_i = \frac{1}{n_i} (R_i)^{(2/3)} \sqrt{S_i} \quad (11)$$

where V_i = flow velocity at grid cell i (m/s); n_i = Manning's roughness at grid cell i ; S_i = longitudinal slope at grid cell i (m/m); R_i = hydraulic radius at grid cell i (m/m).

It should be noted that slope calculations are done along flow directions, and not using a roving window approach, in order to provide unbiased estimate of the slope (Dunn and Hickey, 1998; Hickey, 2000). Figure 5 shows the velocity contours using Equation (11) based on the 2-predictors model as an example. Dividing the flow length by the velocity yields the travel time through a grid cell:

$$t_{ci} = \frac{n_i}{60V_i} l_i = Weight_i \times l_i \quad (12)$$

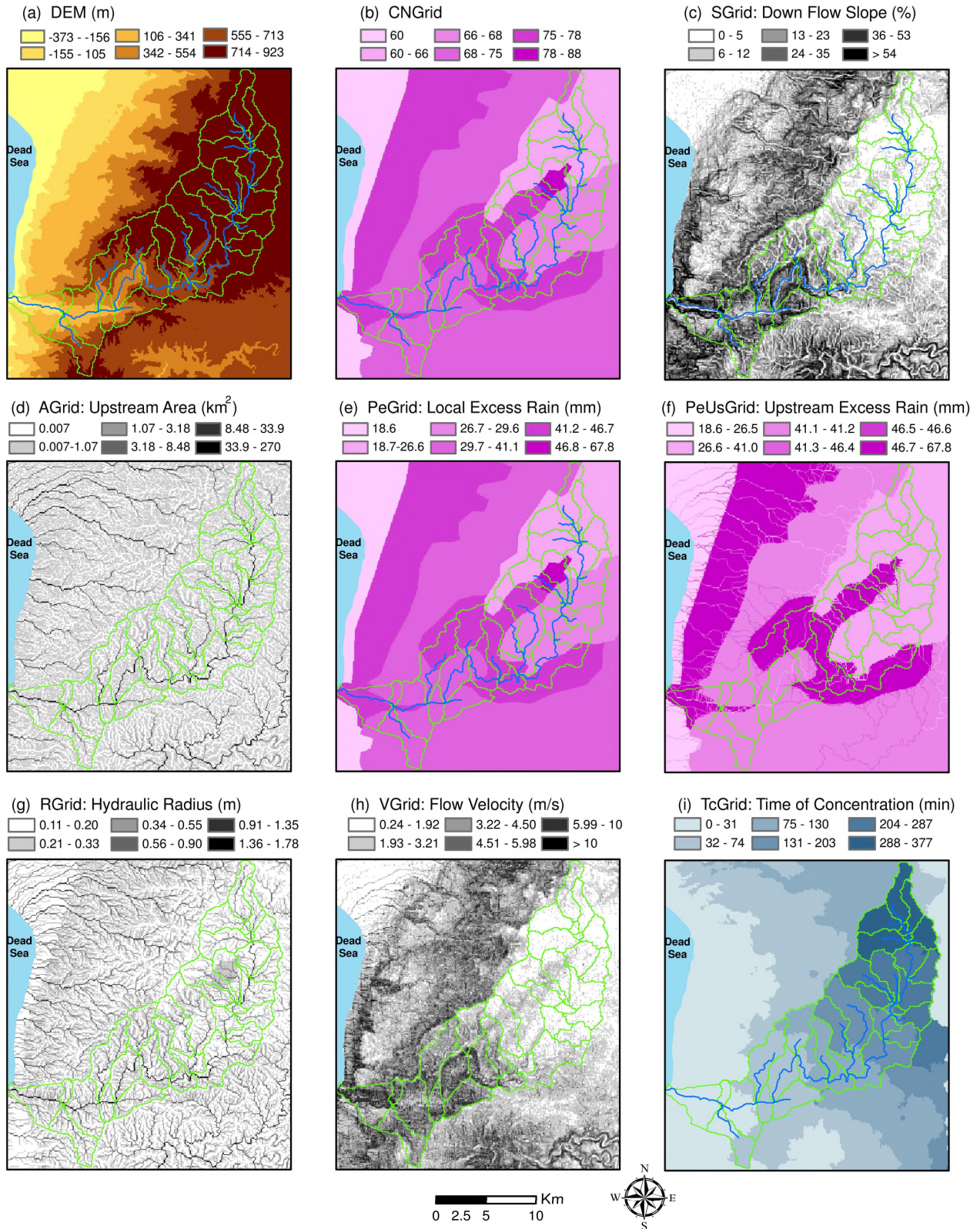


Figure 7. Example of grid-based calculations of the time of concentration for Wadi Zerqa Mai'n (Region 3) using the 2-predictors stream power model. (a) and (b) are inputs while (i) is the final output. All intermediate grids are temporary unless specified else ($n = 0.04$).

where t_{ci} is the travel time through grid cell i in minutes and l_i is the travel length in meters (i.e., the cellsize for the orthogonal directions and 1.414 cellsize for the diagonal directions). The linear relation between t_{ci} and l_i ensures that DEMs of different resolutions for the same area yield close results. The travel time from the grid cell to the watershed outlet Tc_i (time of concentration of this grid cell at the outlet) can be obtained by summing Equation (12) along all downstream grid cells in the flow direction path:

$$Tc_i = \sum_i^{outlet} t_{ci} = \sum_i^{outlet} Weight_i \times l_i \quad (13)$$

Equation (13) is solved using the FlowLength function by using the spatially varied $Weight_i$ (defined in Equation 12) to calculate a time of concentration grid (i.e., TcGrid). The Tc-Grid is a grid in which each cell is given the value of its travel time to the outlet. Figure 6 presents a flow chart of the GIS module.

6. Demonstration Cases

Figure 7 presents examples for the UsAreaGrid, PeGrid, PeUsGrid, Rgrid, VGrid, and TcGrid for Wadi Zerqa Mai'n east of the Dead Sea (region 3, Jordan) for a storm of 100 mm total daily rainfall depth. Wadi Zerqa Mai'n is characterized with mild slopes in its upper catchments to relatively steep slopes closer to the Dead Sea (area = 274 km², length = 60 km). Note that a spatially constant Manning's $n = 0.04$ is used. A spatially variable Manning roughness can be easily used in a similar way as done with the curve number. In order to fully demonstrate the functionality of the technique, the technique is run for different rainfall depths on Wadi Zerqa Mai'n. The same procedure is repeated for Wadi Al-Mashkak from Menia in Upper Egypt (area=488 km², length=68 km) which is characterized with very mild slopes. Figure 8 shows the calculated times of concentration for the two watersheds at different storm total rainfall depths. The figure explains the advantage of modeling a storm-dependent hydraulic radius especially if flood forecasting is to be involved. Additional advantages exist in the computation simplicity and accuracy. The technique does not require hard disk space and is not memory intensive. Grids are temporary grids that are automatically deleted from the computer hard disk by GIS unless specified else by the user. In addition, the developed GIS technique is of excellent run time (within a few seconds).

7. Discussion and Conclusions

The hydraulic radius is a measure of the flow efficiency of a river reach. The core hypothesis of this research implies that a river tries to maintain its flow efficiency through local reaches (i.e., at constant discharge). Accordingly, rivers try to follow the easiest way to maintain their efficiencies locally. This is accomplished through vertical erosion in mountainous reaches and lateral erosion/meandering in alluvial reaches. This

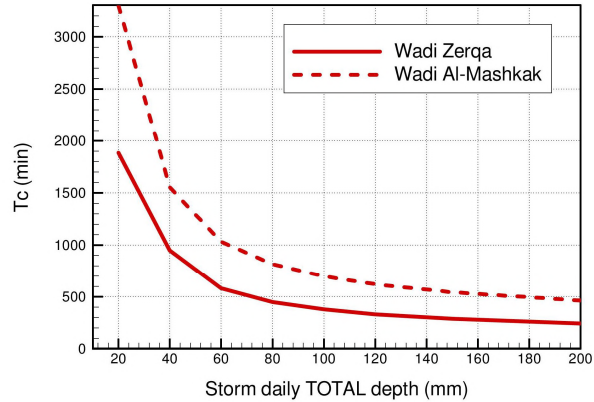


Figure 8. The calculated times of concentration for Wadi Zerqa Mai'n and Wadi Al-Mashkak for different storm daily TOTAL rainfall depths ($n = 0.04$).

makes the hydraulic radius less sensitive to any local abrupt geomorphologic changes in width or depth. In addition, and from the hydraulics point of view, using the hydraulic radius (cross sectional area/wetted perimeter) eliminates some geomorphologic interactions between width, depth and slope and hence leads to a more stable hydraulic radius value at a constant discharge. Accordingly, a much better fit is achieved in the stream power fitting. This stability gives the hydraulic radius (as a response in the stream power laws) a strong advantage over the typical geomorphologic variables (i.e., width, depth, and slope). To explain this, consider two successive river reaches where slope changes from steep to mild. The steep reach (normally flows through rocky mountainous terrain) has small channel width and depth compared to the next mild-slope reach (normally alluvial). The change in the hydraulic radius between the two reaches should be minimum compared to the changes in bed width, depth, or slope (i.e., velocity). The same idea applies to the deep-to-wide transition of a hydraulic cross section and vice versa. This means that the hydraulic radius should remain relatively (as compared to the bed width or depth) constant as long as the discharge is constant. The findings of this research strongly support the above hypothesis. However, similar studies are required in regions with more available rainfall-runoff data and in regions of different hydro-geomorphologic configurations (i.e., the grassed and forested configurations in Canada, Europe, and tropical regions). This is strongly recommended for future studies to check the stream power hypothesis of the hydraulic radius in these regions and to reach to any possible new parameterization.

The use of modeled discharges instead of measured discharges in fitting the stream power laws may be criticized as a source of bias. The hydrologic modeling done in this research tried to minimize bias as much as possible through the use of previously calibrated hydrologic parameters. In addition, since the cases used in regression are characterized with large diversity in the hydrologic parameters and storm depths, the differences between the calculated discharges and actual discharges can be assumed to follow a normal distribution with zero mean with some degree of confidence. However, the verification ca-

ses presented in section 4.2 and in Gad (2013) provide some evidences that the developed formulas are unbiased. Additional future studies shall fully evaluate their performance.

The main advantages of the developed technique are its simplicity and flexibility that suit different water resources applications in semiarid regions. This is because the technique requires data that is readily available. In addition, the calculated travel times are storm dependent giving the ability to simulate the dynamics with minimum data and processing requirements. The developed GIS technique can supply grids of time of concentration and flow velocity to the real-time rainfall-runoff models for the purpose of flood forecasting and real-time operation of flood control structures. On the other side, it can also be implemented for water quality assessments.

References

- Abdo, G., Sonbol, M., and Willems, P. (2009). Flood Frequency Analysis of the Eastern Nile Rivers. Technical paper, FRIEND/ Nile Project, UNESCO Cairo office.
- Abdelrahman, H. (1992). Water resources potentialities of the Suez Gulf region, representative catchment in Sudr area, Sinai. MSc thesis, Department of Civil Engineering, Cairo University, Cairo, Egypt.
- Ajward, M.H., and Muzik, I. (2000). A spatially varied unit hydrograph model. *J. Environ. Hydrol.*, 8, 1-8. <http://www.hydroweb.com/jeh/jeh2000/ajward.pdf>
- Arora, V., Seglenieks, F., Kouwen, N., and Soulis, E. (2001). Scaling aspects of river flow routing. *Hydrol. Process.*, 15, 461-477. <http://dx.doi.org/10.1002/hyp.161>
- Carlston, C.W. (1969). Downstream variations in the hydraulic geometry of streams: special emphasis on mean velocity. *Am. J. Sci.*, 267, 499-509. <http://dx.doi.org/10.2475/ajs.267.4.499>
- Chiang, S., Tachikawa, Y., and Takara, K. (2004). Rainfall-runoff simulation by using distributed instantaneous unit hydrograph derived from applying flow accumulation. *Annu. J. Hydraul. Eng.*, 48, 1-6. <http://dx.doi.org/10.2208/prohe.48.1>
- DAR (2006). Design of Shendi Al-Mattama bridge over the Nile, Hydraulic design report, Dar Al Handasah (Shair and Parteners), Cairo, Egypt.
- Dervos, N., Baltas, E.A., and Mimikou, M.A (2006). Rainfall simulation in an experimental basin using GIS methods. *J. Env. Hydrol.*, 14, 1-14. <http://www.hydroweb.com/jeh/jeh2006/baltas.pdf>
- Du, J.K., Xie, H., Hu, Y.J., Xu, Y.P., and Xu, C.Y. (2009). Development and testing of a new storm runoff routing approach based on time variant spatially distributed travel time method. *J. Hydrol.*, 369(1-2), 44-54. <http://dx.doi.org/10.1016/j.jhydrol.2009.02.033>
- Dunn, M., and Hickey, R. (1998). The effect of slope algorithms on slope estimates within a GIS. *Cartography*, 27 (1), 9-15. <http://dx.doi.org/10.1080/00690805.1998.9714086>
- El-Sayed, E.A., and Habib, E. (2008). Advanced technique for rainfall-runoff simulation in arid catchments Sinai. Egypt, 3rd International Conference on Water Resources and Arid Environments.
- Environmental Systems Research Institute (ESRI) (2006). Hydrologic Modeling with Arc-Hydro Tools.1, ESRI Press.
- Fahmi, A.H. (1992). Frequency analysis of rainfall and prediction of runoff in catchment areas. MSc thesis, Department of Civil Engineering, Ain Shams University, Cairo, Egypt.
- Finlayson, D.P., and Montgomery, D.R. (2003). Modeling large-scale fluvial erosion in geographic information systems. *Geomorphology*, 53, 147-164. [http://dx.doi.org/10.1016/S0169-555X\(02\)00351-3](http://dx.doi.org/10.1016/S0169-555X(02)00351-3)
- Gad, M.A. (1996). Hydrology of Wadies in Sinai. MSc thesis, Department of Civil Engineering, Ain Shams University, Cairo, Egypt.
- Gad, M.A. (2013). A useful automated rainfall-runoff model for engineering applications in semi-arid regions. *Comput. Geosci.*, 52, 443-452. <http://dx.doi.org/10.1016/j.cageo.2012.09.023>
- Gross, E.J., and Moglen, G.E. (2007). Estimating the hydrological influence of Maryland state dams using GIS and the HEC-1 model. *J. Hydrol. Eng.*, 12 (6), 690-693. [http://dx.doi.org/10.1061/\(ASCE\)1084-0699\(2007\)12:6\(690\)](http://dx.doi.org/10.1061/(ASCE)1084-0699(2007)12:6(690))
- Hickey, R. (2000). Slope angle and slope length solutions for GIS. *Cartography*, 29 (1), 1-8. <http://dx.doi.org/10.1080/00690805.2000.9714334>
- Howard, A.D. (1998). Long profile development of bedrock channels: interaction of weathering, mass wasting, bed erosion, and sediment transport. In: Tinkler, K.J., Wohl, E.E. (Eds.), *Rivers over Rocks: Fluvial Processes in Bedrock Channels*. American Geophysical Union, Washington, DC, 297-319. <http://dx.doi.org/10.1029/GM107p0297>
- Hydrologic Engineering Center (HEC) (1973). HEC-1 flood hydrograph package user Manual, U.S. Army Corps of Engineers, Davis, California.
- Hydrologic Engineering Center (HEC) (2010). HEC-GeoHMS: Geospatial hydrologic modeling extension, User's manual, Ver.5. US Army Corps of Engineers.
- Jain, M., Kothiyari, U., and Rangaraju, K. (2004). A GIS based distributed rainfall-runoff model. *J. Hydrol.*, 299(1-2), 107-135. <http://dx.doi.org/10.1016/j.jhydrol.2004.04.024>
- Kirpich, Z.P. (1940). Time of concentration of small agricultural watersheds, *Civil Engineering* 10(6), 362.
- Klien, M. (1999). The formation and disappearance of a delta at the El-Arish river mouth. *The Hydrology-Geomorphology Interface: Rainfall, Floods, Sedimentation, Land Use* (Proceedings of the Jerusalem Conference, May 1999). IAHS Publ. no. 261, 2000.
- Kobor, J.S., and Roering, J.J. (2004). Systematic variation of bedrock channel gradients in the central Oregon Coast Range: implications for rock uplift and shallow landsliding. *Geomorphology*, 62, 239-256. <http://dx.doi.org/10.1016/j.geomorph.2004.02.013>
- Kouwen, N., Soulis, E.D., Pietroniro, A., Donald, J., and Harrington, R.A. (1993). Grouping response units for distributed hydrologic modeling. *J. Water Resour. Manage. Plann.*, 119(3), 289-305. [http://dx.doi.org/10.1061/\(ASCE\)0733-9496\(1993\)119:3\(289\)](http://dx.doi.org/10.1061/(ASCE)0733-9496(1993)119:3(289))
- Leopold, L.B., and Maddock, T. (1953). The hydraulic geometry of stream channels and some physiographic implications. Professional Paper 252, US Geological Survey, Washington, DC.
- Maidment, D. (1993). Developing a spatially distributed unit hydrograph by using GIS. *HydroGIS 93*, edited by K. Kovar and H. P. Nachtnebel, Publ. 211, 181-192, Int. Assoc. of Sci. Hydrol., Wallingford, Engl., U.K.
- Manning, R. (1891). On the flow of water in open channels and pipes. *Transactions of the Institution of Civil Engineers of Ireland*, 20, 161-207.
- Montgomery, D.R., and Gran, K.B. (2001). Downstream variations in the width of bedrock channels. *Water Resour. Res.*, 37, 1841-1846. <http://dx.doi.org/10.1029/2000WR900393>
- Nyarko, B.K. (2002). Application of a rational model in GIS for flood risk assessment in Accra, Ghana. *J. Spatial Hydrol.*, 2 (1). <http://www.spatialhydrology.net/index.php/JOSH/article/download/7/6>
- Overton, D.E., and Meadows, M.E. (1976). *Stormwater Modeling*. New York Academic Press.
- Rao, A.R., and Delleur, J.W. (1974). Instantaneous unit hydrographs, peak discharges, and time lags in urban areas. *Hydrol. Sci. Bull.*, 19 (2), 185-198. <http://dx.doi.org/10.1080/02626667409493898>
- Seo, D.J., and Smith, J.A. (1992). Radar based short term rainfall prediction. *J. Hydrol.*, 131, 341-367. <http://dx.doi.org/10.1016/00>

- 22-1694(92)90225-K.
- Sharifi, S., and Hosseini, S.M. (2011). Methodology for identifying the best equations for estimating the time of concentration of watersheds in a particular region. *J. Irrig. Drain. Eng.*, 137(11), 712-719. [http://dx.doi.org/10.1061/\(ASCE\)IR.1943-4774.0000373](http://dx.doi.org/10.1061/(ASCE)IR.1943-4774.0000373)
- Sircar, J.K., Ragan, R.M., Engman, E.T., and Fink, R.A. (1991). A GIS based geomorphic approach for the digital computation of time-area curves. In: Proceedings of the ASCE Symposium on Remote Sensing Applications in Water Resources Engineering.
- Sklar, L., and Dietrich, W.E. (1998). River longitudinal profiles and bedrock incision models: stream power and the influence of sediment supply. In: Tinkler, K.J., Wohl, E.E. (Eds.), *Rivers over Rock: Fluvial Processes in Bedrock Channels*. American Geophysical Union, Washington, DC, 237-260. <http://dx.doi.org/10.1029/GM107p0237>
- Sorman, A.U., Abdulrazzak, M.J., and Elhames, A.S (1990). Rain-fall-runoff modeling of a microcatchment in the western region of Saudi Arabia. *Hydrology in Mountainous Regions. I-Hydrological Measurements; the Water Cycle (Proceedings of two Lausanne Symposia, August 1990)*. IAHS Publ. no. 193.
- Stock, J., and Montgomery, D.R. (1999). Geologic constraints on bedrock river incision using the stream power law. *J. Geophys. Res.*, 104, 4983-4993. <http://dx.doi.org/10.1029/98JB02139>
- Soil Conservation Service (SCS) (1972). *National Engineering Handbook*, section 4, Hydrology. U. S. Dept. of Agriculture. Available from U. S. Government Printing Office Washington, D.C.
- Soil Conservation Service (SCS) (1973). A method for estimating volume and rate of runoff in small watersheds, U. S. Dept. of Agriculture.
- Thomas, W.O. Jr., Monde, M.C., and Davis, S.R. (2000). Estimation of time of concentration for Maryland streams. Transportation Research No.1720, Transportation Research Board, National Research Council, National Academy Press, Washington, DC, 95-99.
- Tsanis, I.K., and Gad, M. (2003). A GIS Methodology for the Analysis of Weather Radar Precipitation Data. *J. Hydroinf.*, 5(2), 113-126. <http://www.iwaponline.com/jh/005/0113/0050113.pdf>
- Walters, M.O. (1990) Transmission losses in arid region. *J. Hydraul. Eng.*, 116 (1), 129-138. [http://dx.doi.org/10.1061/\(ASCE\)0733-9429\(1990\)116:1\(129\)](http://dx.doi.org/10.1061/(ASCE)0733-9429(1990)116:1(129))
- Wanielista, M., Kersten, R., and Eaglin, R. (1997). *Hydrology: water quantity and quality control*, John Wiley & Sons, 2nd ed.
- Whipple, K.X., and Tucker, G.E. (1999). Dynamics of the stream-power river incision model: implications for height limits of mountain ranges, landscape response timescales, and research needs. *J. Geophys. Res.*, 104, 17661-17674. <http://dx.doi.org/10.1029/1999JB900120>